Hindawi
International Journal of Antennas and Propagation
Volume 2023, Article ID 5344999, 13 pages
https://doi.org/10.1155/2023/5344999

Research Article

A Triband Compact Antenna for Wireless Applications

D. Allin Joe [1] **and Thiyagarajan Krishnan** [2]

[1]*Department of Electronics and Communication Engineering, Kumaraguru College of Technology, Coimbatore, Tamil Nadu, India*
[2]*Department of Electronics and Communication Engineering, PSG College of Technology, Coimbatore, Tamil Nadu, India*

Correspondence should be addressed to D. Allin Joe; allinjoe.d.ece@kct.ac.in

Received 28 June 2023; Revised 22 July 2023; Accepted 25 August 2023; Published 2 September 2023

Academic Editor: Sreenath Reddy Thummaluru

This paper presents the implementation of a triple band microstrip patch antenna based on modified split ring resonator (SRR) and modified complementary split ring resonator (CSRR) as defected ground plane. The antenna is designed in a FR4 substrate of dielectric constant 4.4 with dimensions as 35 mm × 35 mm × 1.6 mm that comprises a total designed antenna volume of 1960 mm^3. Multiband operation is introduced in the antenna through multiple resonators that are introduced in the patch. Impedance matching was provided with the help of partial ground plane and modified SRR in patch. The simulation performance of the antenna is verified using high frequency structural simulator (HFSS) software. The designed antenna resonates at 2.8 GHz, 5.8 GHz, and 6.9 GHz for the application requirements of WiMAX, ISM, and Sub-7 GHz wireless communication. The antenna is fabricated as printed circuit board (PCB) format, and its return loss characteristics are measured using a vector network analyser (VNA). The measurement results of the proposed triband antenna are in good agreement with simulated return loss characteristics.

1. Introduction

In recent years, there is an increasing demand for the usage of wireless devices in many of the medical and industrial applications. The wireless devices simplified the communication in the indoor environment and maintained connectivity for a balanced work style. Antenna is the important module used in all wireless devices. The technological growth in very large-scale integration (VLSI) design and fabrication methodologies considerably reduced the size of the wireless devices. Therefore, size of the antenna must be as small as possible in proportion with the size of the wireless device. The microstrip patch antenna suits the requirements of the recent era wireless devices since it is conformal in nature [1].

Rectangular patch antenna is the fundamental antenna structure over which a slight modification is done to achieve the desired radiation characteristics. Different configurations of slots can be introduced in the patch and ground plane of the antenna to achieve resonance at many frequencies [2, 3]. The electrical size of the antenna can be decreased by embedding a metamaterial in the middle of the substrate of the patch antenna that results in miniaturization of antenna that suits for the thin communication devices [4]. The performance of the patch antenna can be enhanced by using a combination of defective ground plane and metamaterial [5]. The antenna parameters can be improved by loading additional elements in the patch and ground plane. The antenna efficiency can be increased by using shorting pins [6]. The introduction of defected ground structure (DGS) over a stub loaded slot antenna will result in a wider bandwidth [7]. The edge coupled SRR parasitic elements are loaded in a fractal antenna to improve the impedance matching parameters which in turn increases the operational bandwidth of the antenna [8].

The main disadvantage of a microstrip patch antenna is its narrow band characteristics. The microstrip patch antenna needs to be tuned to multiband and wide band requirements for real-time applications. Predominantly, SRR structures and CSRR structures can be used either in patch

or ground plane to achieve multiband requirements. The multiband needs to be tuned to the desired frequencies for proper operation of the wireless devices. The modification of ground plane and SRR and CSRR structures is performed to achieve the desired frequencies [9, 10]. The compactness of the designed antenna shall be improved by introducing a combination of SRR, CSRR, and substrate integrated waveguide (SIW) in rectangular patch antenna that is designed based on a composite right/left-handed transmission line [11].

In [12], square ring slots are created in ground plane as DGS to attain triple band characteristics. The effect of the resonant frequency over the variation in the deformation of the ground plane is analysed, and a mathematical model is constructed for the relationship in [13]. The impact of removing the ground plane partially over the radiation characteristics of the carpet fractal antenna is investigated in [14]. A short-ended metamaterial structure coplanar waveguide (CPW) fed compact antenna using U-shaped and rectangular shaped strip is designed for a maximum radiation efficiency is presented in [15]. Square CSRR structure is introduced in the ground plane of a rectangular patch for size reduction in industrial, scientific, and medical (ISM) band applications [16, 17]. The antenna can be made compact by introducing square stub, meandered lines, a reverse L-shaped resonator, and a ring resonator and arranging them in the form of composite right/left transmission line [18]. Power divider used to distribute the power for antennas is designed for triple band in a way like that of a patch antenna for three frequency bands [19].

The recent innovations in Worldwide Interoperability for Microwave Access (WiMAX) standard makes it a more viable option in the field of wireless communication during this wireless Internet era. It is a fourth-generation communication standard that operates at a frequency of 2.8 GHz [20]. ISM band is a universal unlicensed band used for short range communication among wireless devices. It is a very useful band for the wireless consumers and commercial applications that operate at a frequency of 5.8 GHz [21]. C Band includes the spectrum in the range of 4 GHz to 8 GHz which includes several communication standards [22]. Sub-7 GHz band used in the deployment of the fifth generation has improved latency and better coverage characteristics with a frequency range of 6 GHz to 7.1 GHz [23].

This work mainly concentrates on the design and analysis of a compact triband antenna for the WiMAX, ISM, and Sub-7 GHz band wireless applications. Section 2 discusses the design methodology followed in the proposed work. The parametric analysis of the proposed antenna is carried out in Section 3. The measured radiation pattern and gain results of the fabricated antenna in an anechoic chamber are discussed in Section 4 along with a comparison of the works in the literature. The final section concludes the proposed work.

2. Structural Synthesis of Multiband Antenna

The design process of multiband antenna originates from the formation of conventional single band rectangular patch antenna. The multiband operation of the patch antenna is realized by using the complementary SRR-based structure. The further improvement in the impedance matching characteristics of the antenna is achieved with the support from CSRR-based DGS techniques. The modified SRR structure in the patch and the modified CSRR structure as well as the partial ground plane in the ground plane account for miniaturization of the designed antenna.

2.1. Conventional Basic Rectangular Patch Antenna. A square-shaped FR4 substrate with dimensions $35\,\text{mm} \times 35\,\text{mm} \times 1.6\,\text{mm}$ is selected. The rectangular shaped patch with dimensions $29\,\text{mm} \times 20\,\text{mm}$ is created over the FR4 substrate. Microstrip feed mechanism is used to excite the basic antenna structure.

2.2. Modified Split Ring Resonator Structure of Patch. The modified split ring resonator structure is introduced in the patch to minimize the size of antenna. SRR structure increases the effective length of the antenna which confines the antenna to radiate at lower frequencies. The basic form of SRR consists of rings that are made of copper or any other conductive material with a small gap between them as shown in Figure 1. The SRR rings may be of any shape such as circle, square, etc. The rings in SRR represent an inductor since they are made of copper or other conductive materials. The combination of SRR rings and the small gap between the SRR rings represents the capacitor. The SRR rings are made of the conducting material which denotes the conductive plates of the capacitor, and the gap between the SRR rings is made from FR4 dielectric material to represent the dielectric filled gap in the capacitor.

Let the length of a side be l_1 for the inner square loop of SRR structure. Let c be the speed of light in a free space environment and ε_{eff} be the effective dielectric constant which depends on the material used for fabrication of the SRR structure. The resonant frequency F_1 generated by the inner square loop of SRR is given by [24].

$$F_1 = \frac{c}{2l_1\sqrt{\varepsilon_{\text{eff}}}}. \tag{1}$$

Let the length of a side be l_2 for the outer square loop of SRR. The resonant frequency F_2 generated by the outer square loop of SRR structure is given by

$$F_2 = \frac{c}{2l_2\sqrt{\varepsilon_{\text{eff}}}}. \tag{2}$$

The electrical length of the outer loop of SRR structure is longer than the inner loop of SRR structure. The resonant frequency generated by the outer loop of SRR structure is lower than the resonant frequency generated by the inner loop of SRR structure. Since both the outer loop and inner loop of SRR structure are very close to each other, the coupling effect will create a shift in F_1 and F_2 resonant frequencies. The evolution of the patch antenna with SRR structure is shown in Figure 2. The initiator of the patch antenna with SRR structure is a half patch which is shown in Figure 2(a). The initiator is a simple

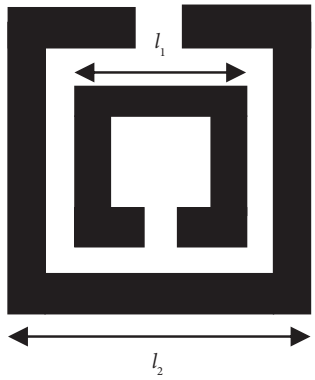

Figure 1: Split ring resonator structure.

rectangular patch antenna which shall be represented as a combination of a resistor, capacitor, and inductor components. A defective microstrip structure (DMS) is introduced at the middle of the initiator, and the initiator is divided into equal upper and lower parts as shown in Figure 2(b). The created structure increases the capacitance effect of the patch due to the presence of dielectric gap between two conductive materials. The equally divided initiator parts are etched in the middle to resemble a square ring resonator. A rectangular ring resonator is created through the middle of the upper and lower square ring resonators as shown in Figure 2(c). This structure increases the inductance effect of the patch. The inner ring of the resonator is formed in the upper square ring resonator and the rectangular square ring resonator as shown in Figure 2(d). Each ring can generate different frequencies, and their effect is combined to produce the desired resonant frequencies. The split is induced in the middle part of the square and rectangular ring resonators to resemble like a SRR structure as shown in Figure 2(e) which is the finalized patch antenna structure.

Figure 3 shows the geometry of the patch antenna with SRR structure, and its dimensions are given in Table 1. Figure 4 shows the patch antenna with SRR structure created in HFSS software. The total length of the antenna is increased by introducing the SRR structure in the initiator. The increase in the antenna length in turn increases the current paths in the surface of patch. The current paths introduced in the additional length of the antenna generate multiple resonant frequencies. The return loss plot of the patch antenna with SRR structure is shown in Figure 5. The patch antenna with SRR structure has three resonant frequencies. The lower order resonant frequency 1.9 GHz has 13.04 dB return loss with a narrow bandwidth of 69 MHz, the next order resonant frequency 5.5 GHz has 10.81 dB return loss with a very narrow bandwidth of 17 MHz, and the higher order resonant frequency 8.7 GHz has 15.44 dB return loss with a bandwidth of 204 MHz. The three obtained resonant frequencies can be modified to the desired frequencies by altering the size of the ground plane of the patch antenna with SRR structure.

2.3. Partial Ground Plane Structure. The partial ground plane structures are used instead of the full ground plane to improve the return loss characteristics in the microstrip patch antenna. The energy stored in the ground plane substrate is reduced by using the partial ground plane structure, and it reduces the diffraction of the surface waves along the edges of the ground plane of the antenna. To improve the return loss characteristics, the size of the ground plane of the proposed patch antenna structure is adjusted. The different ground plane considerations for the patch antenna with SRR structure is shown in Figure 6.

Figure 7 shows the return loss performance of the patch antenna with SRR structure for various values of the ground plane length (L). The resonant frequencies generated by varying the length of the ground plane (L) of the patch antenna with SRR structure and their associated return loss values are presented in Table 2. When the ground plane size is reduced to 3 $L/4$, the proposed patch antenna structure radiates for one resonant frequency with return loss less than 10 dB, but there are two resonant frequencies with return loss less than 10 dB when the ground plane size is reduced to $L/2$ and three resonant frequencies with return loss less than 10 dB exists for the ground plane size of $L/4$. The $L/4$ sized ground plane is selected for further optimization since it has three resonant frequencies with good return loss characteristics than L, 3 $L/4$, and $L/2$ ground planes.

2.4. Modified Complementary Split Ring Resonator (CSRR) Structure in Partial Ground Plane Structure. CSRR structures are the dual of SRR structures. In the conducting patch, the CSRR structures are etched as shown in Figure 8(a). The conducting part within the CSRR structure increases the inductance effect of the designed antenna. The capacitance effect is introduced in the split gap of the CSRR rings. The equivalent circuit of CSRR resembles an LC circuit, and the resonant frequency of CSRR (F_{CSRR}) structure is as follows:

$$F_{\text{CSRR}} \propto \frac{1}{\sqrt{\text{LC}}}. \tag{3}$$

As shown in equation (3), the resonant frequency of CSRR structure is inversely proportional to the inductance and capacitance values created by it. By using the CSRR structure in the patch antenna, the resonant frequency of the patch antenna will be shifted due to the impact of the coupling effect that happens between the gap of CSRR rings as well as the split gap in CSRR rings. In the designed antenna, the CSRR shape can be introduced in the $L/4$ ground plane patch antenna structure to improve the return loss and bandwidth characteristics. This leads to a shift in the resonant frequencies tabulated in Table 2. As the aim of the work is to increase the return loss and bandwidth characteristics of the antenna, the shifting of resonant frequencies by introducing the CSRR structure can be neglected by eliminating the coupling effect between the CSRR structures. The coupling effect is mainly concentrated in the split gap in CSRR rings as well as between the CSRR rings. Hence, the CSRR structure shown in Figure 8(a) needs to be modified to achieve better return loss and bandwidth characteristics of the proposed antenna.

The inner ring in the CSRR structure is removed as shown in Figure 8(b) since the presence of the inner ring will shift the resonant frequency values as tabulated in

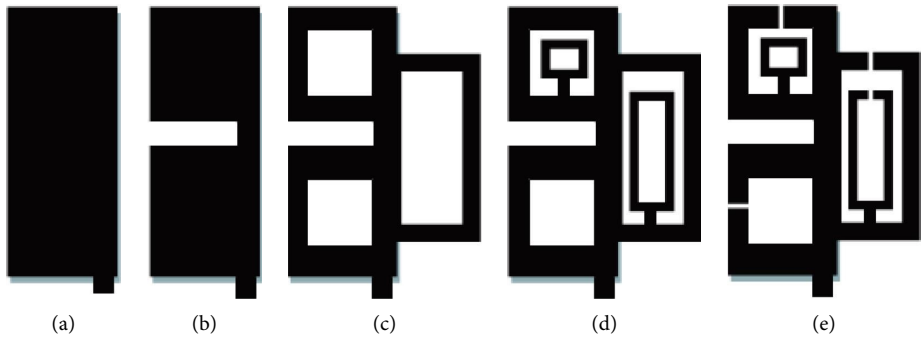

Figure 2: Evolution of the patch antenna with SRR structure.

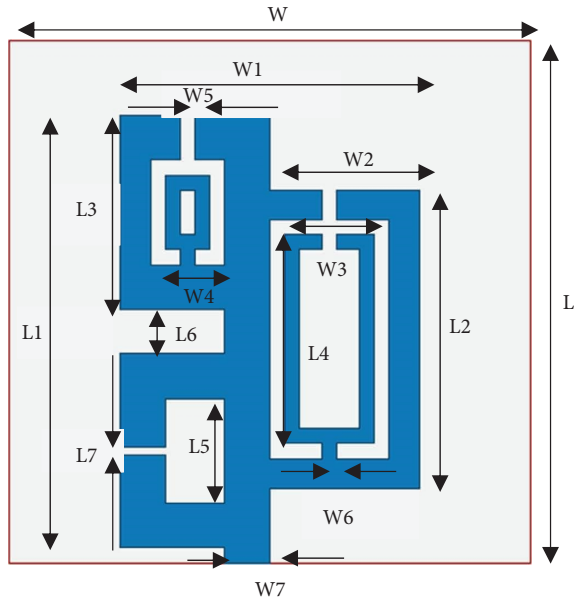

Figure 3: Geometry of the patch antenna with SRR structure.

Table 1: Dimensional parameters of the patch antenna with SRR structure.

Width of patch antenna		Length of patch antenna	
Parameter	Value (mm)	Parameter	Value (mm)
W	35	*L*	35
*W*1	19	*L*1	29
*W*2	10	*L*2	20
*W*3	5	*L*3	13
*W*4	5	*L*4	14
*W*5	1	*L*5	7
*W*6	1	*L*6	3
*W*7	3	*L*7	0.8

Table 2. By removing the inner ring in the CSRR structure, the effect of coupling is reduced to a certain extent. The CSRR structure is further reduced by removing the split in the top of the structure as shown in Figure 8(c) which further reduces the capacitance effect in the CSRR structure. Hence, the effect of coupling by using the CSRR structure can be much reduced by using the modified CSRR structure. Generally, the capacitance effect of the antenna between the two rings and the split gap reduces the electrical size of the antenna and causes a major impact on shifting of the resonant frequencies. By using the modified CSRR structure in the patch antenna with partial ground plane structure will vary the inductance and capacitance values of the antenna structure and alter the radiation characteristics of the partial ground plane structure. The modified CSRR structure is introduced in the ground plane of the designed antenna, and the proposed antenna structure is shown in Figure 9. The slot width of the modified CSRR structure is varied to find the optimal slot width value that provides better return loss and bandwidth characteristics.

2.5. Electric Field Distribution of the Proposed Antenna Structure. The electric field distribution at the specific resonant frequencies is used to find the electric strength in the proposed antenna structure when an external excitation is given. Figure 10 represents the electric field distribution of the proposed antenna structure for the resonant frequencies

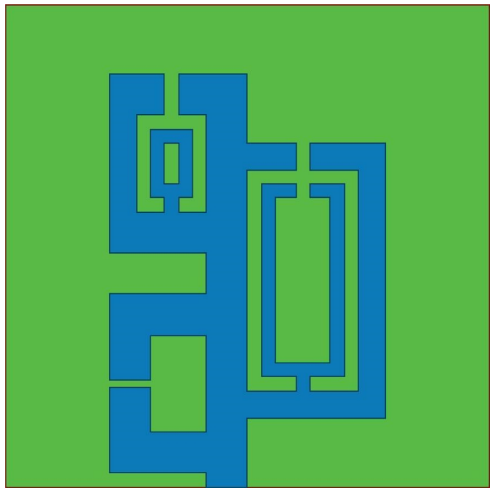

Figure 4: Patch antenna with SRR structure using HFSS.

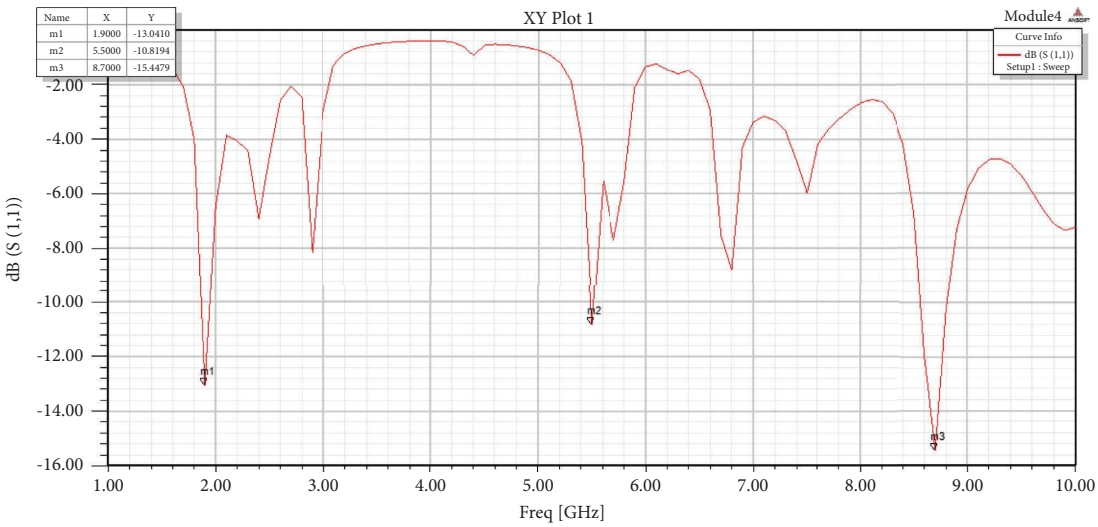

Figure 5: Return loss plot of the patch antenna with SRR structure.

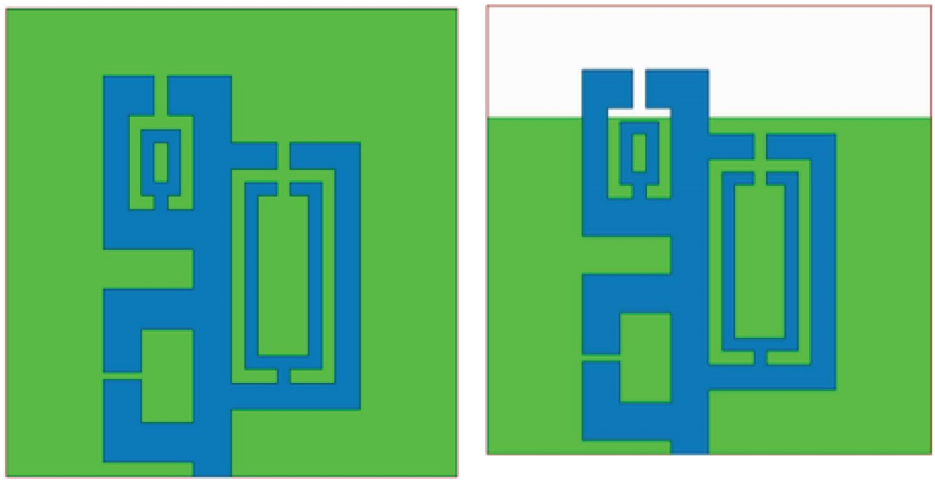

(a) (b)

Figure 6: Continued.

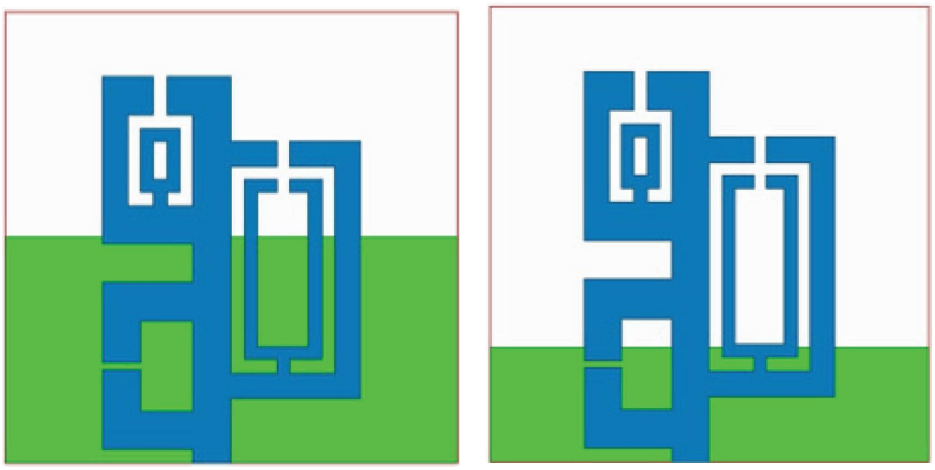

(c) (d)

Figure 6: Ground plane structures of the patch antenna with various ground plane lengths (L) (a) L (b) 3 L/4 (c) L/2 (d) L/4.

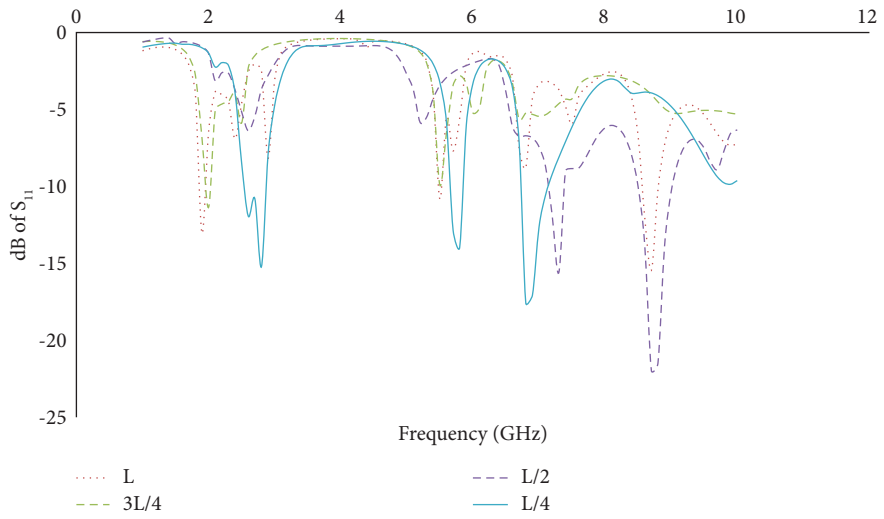

Figure 7: Return loss performance of the SRR patch antenna.

Table 2: Resonant frequency and return loss values by varying ground plane length (L) of the patch antenna with SRR structure.

Ground plane length	First resonance		Second resonance		Third resonance	
	Frequency (GHz)	Return loss (dB)	Frequency (GHz)	Return loss (dB)	Frequency (GHz)	Return loss (dB)
3 L/4	2	11.36	—	—	—	—
L/2	7.3	15.59	8.7	21.96	—	—
L/4	2.8	15.14	5.7	14.77	6.8	22.26

2.8 GHz, 5.8 GHz, and 6.9 GHz. The fundamental frequency 2.8 GHZ is controlled by the gap length $L7$ of the modified SRR structure in the patch which provides the maximum radiation at the fundamental resonant frequency. The resonant frequencies 5.8 GHz and 6.9 GHz are controlled by the modified CSRR structure in the ground plane which generates maximum radiation at those resonant frequencies. Hence, the slot width of the modified CSRR structure is altered to get maximum radiation at 5.8 GHz and 6.9 GHz resonant frequencies.

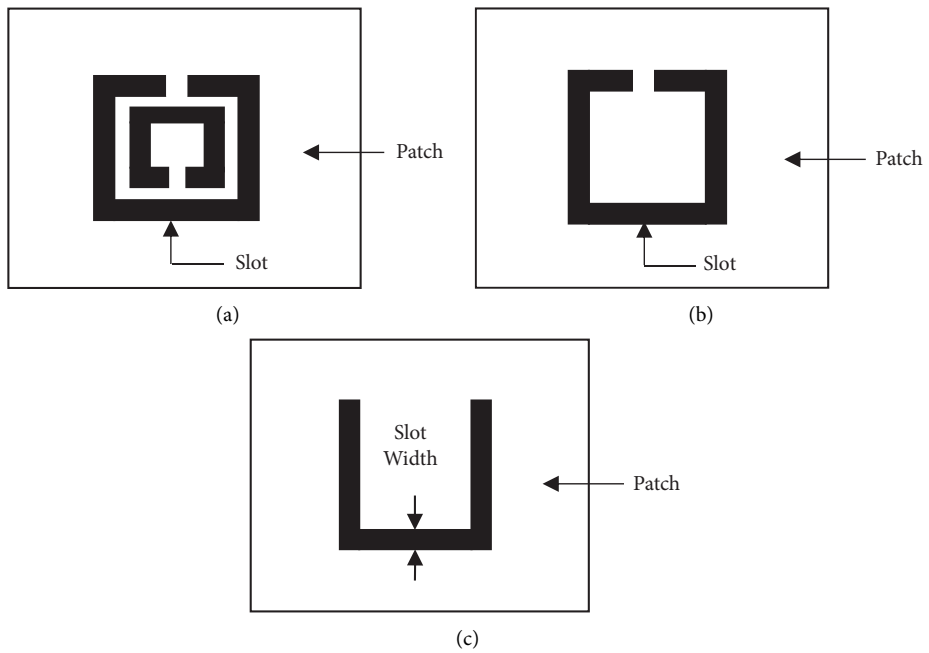

Figure 8: Evolution of the modified CSRR structure.

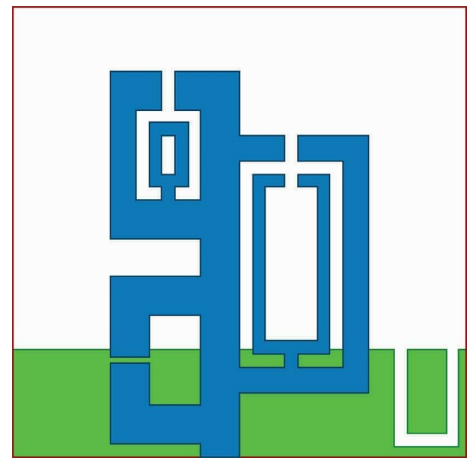

Figure 9: Proposed antenna structure.

3. Parametric Analysis of the Proposed Antenna Structure

3.1. Impact of Slot Width in the Modified CSRR Shape of the Proposed Antenna Structure. The parametric analysis of the proposed antenna structure is performed to evaluate the antenna with optimized dimensions for the desired resonant frequency characteristics. Depending on the results of the parametric study, the proposed antenna structure is simulated using Ansoft HFSS software, fabricated and measured. In Figure 11, the effect of varying the slot width of the modified CSRR structure in the ground plane with respect to the return loss of the proposed antenna structure is shown. Table 3 tabulates the resonant frequency and return loss values by varying the slot width of the modified CSRR structure in the ground plane of the proposed antenna structure. As the slot width dimension increases, the return loss of the resonant frequencies tends to increase to a certain extent and then decreases. By analysing the variation of the return loss characteristics with respect to the change in slot width of the modified CSRR structure in the ground plane of the proposed antenna structure, the slot width of 1 mm is chosen as the optimal value. The proposed antenna structure has a gain of 3.62 dBi at the frequency 2.7 GHz, a gain of 3.48 dBi at the frequency 5.8 GHz, and a gain of 3.22 dBi at 6.8 GHz frequency. The simulated peak gain is 3.62 dBi.

3.2. Radiation Characteristics of the Proposed Antenna Structure. The radiation pattern of the proposed antenna structure is represented by plotting the power radiated from the antenna with respect to spatial direction in a three-

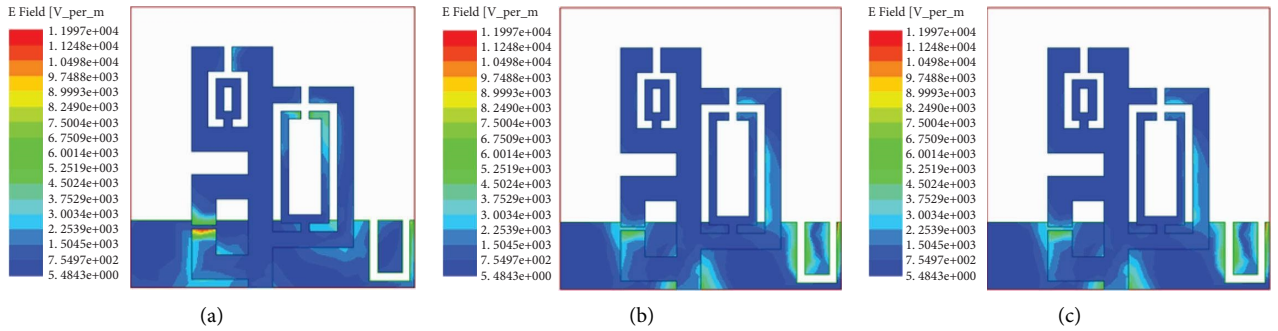

Figure 10: Electric field distribution of the proposed antenna structure (a) 2.8 GHz (b) 5.8 GHz (c) 6.9 GHz.

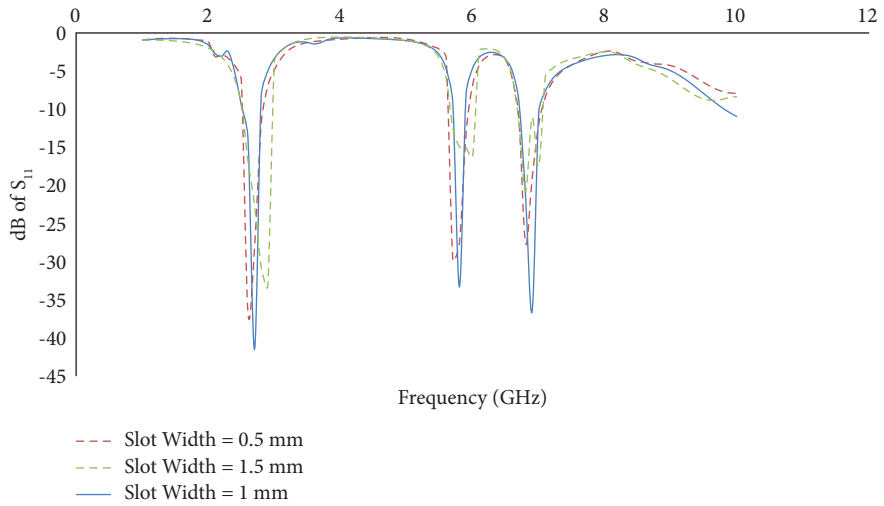

Figure 11: Effect of varying the slot width of the modified CSRR structure in the ground plane of the proposed antenna structure.

Table 3: Performance parameters of the proposed antenna structure.

Slot width (mm)	First resonance		Second resonance		Third resonance	
	Frequency (GHz)	Return loss (dB)	Frequency (GHz)	Return loss (dB)	Frequency (GHz)	Return loss (dB)
0.5	2.6	36.65	5.7	29.64	6.8	27.56
1	2.7	41.44	5.8	33.27	6.9	36.5
1.5	2.9	33.14	6	16.16	6.8	20.76

dimensional system. It reflects the radiation strength of the antenna. The radiation pattern can be used to find the direction in which the antenna radiates more. Slicing the 3D radiation pattern into E-plane and H-plane 2D radiation patterns is much easier to analyse. The radiation pattern and gain of the fabricated antenna are obtained by using an anechoic chamber. Figure 12 displays the E-plane and H-plane radiation characteristics of the proposed antenna structure for the resonant frequencies, 2.8 GHz, 5.8 GHz, and 6.9 GHz. The radiation characteristics at 2.8 GHz illustrate the fundamental operating frequency of the proposed patch antenna structure. There are no nulls in the radiation pattern of the proposed antenna structure at the resonant frequencies, 2.8 GHz, 5.8 GHz, and 6.9 GHz. The obtained radiation pattern at the respective resonant frequencies well suits for WiMAX, ISM, and Sub-7 GHz wireless applications.

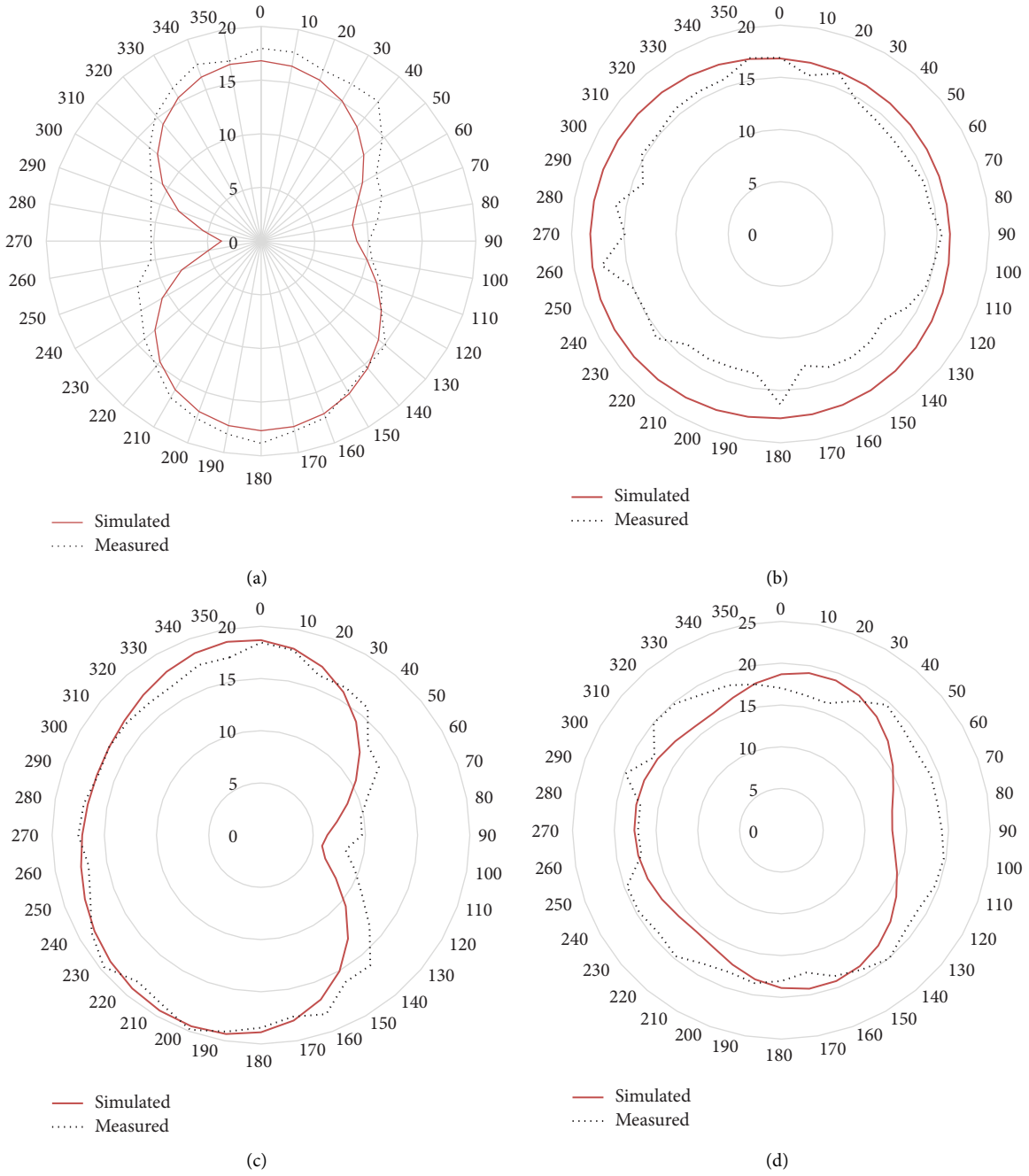

Figure 12: Continued.

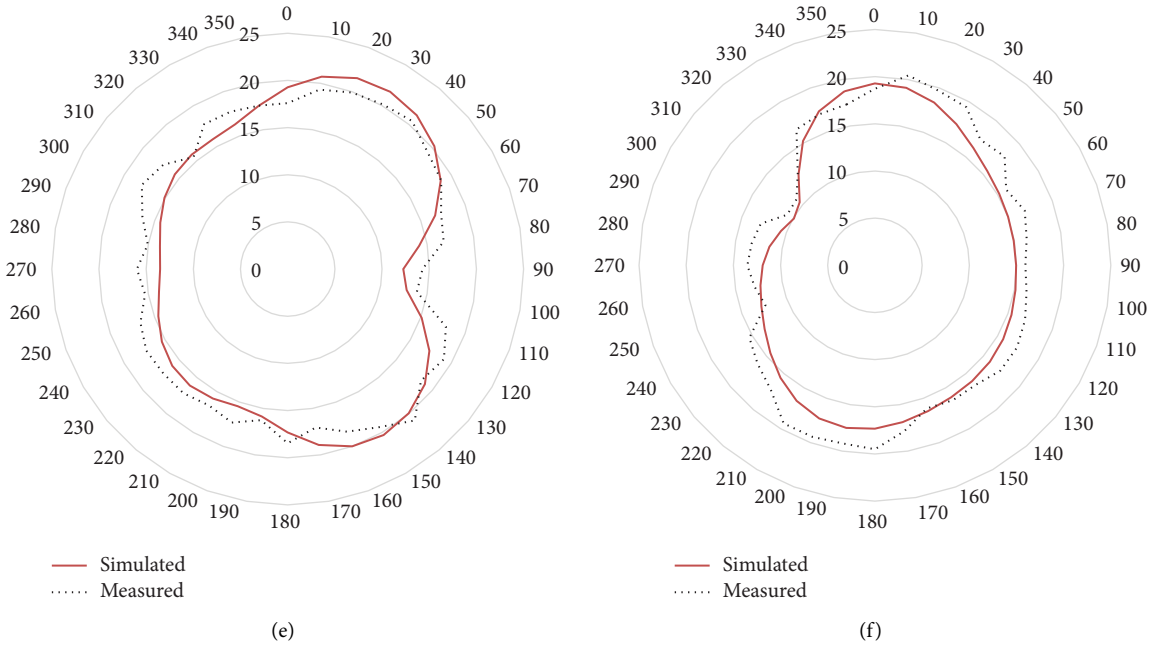

Figure 12: Radiation characteristics of the proposed antenna structure (a) 2.8 GHz E plane (b) 2.8 GHz H plane (c) 5.8 GHz E plane (d) 5.8 GHz H plane (e) 6.9 GHz E plane (f) 6.9 GHz H plane.

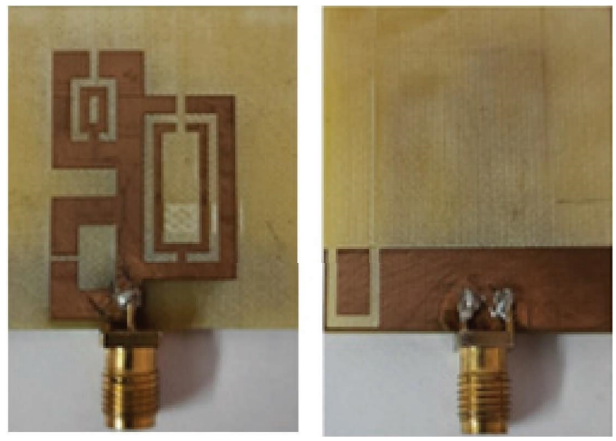

Figure 13: Front and back view of the fabricated antenna structure.

4. Results and Discussion

The proposed triple band antenna structure has been designed using the HFSS software and fabricated over an FR4 substrate. Figure 13 shows the front and back view of the fabricated antenna structure. The fabricated antenna is measured using a N9917A Field Fox Handheld Microwave Analyzer. The measured return loss plot of the fabricated antenna structure is shown in Figure 14. A graphical illustration between the simulated and measured results of the proposed antenna is presented in Figure 15. The resonant frequencies obtained through the simulation done through Ansys HFSS software is slightly shifted to a nearby higher resonant frequencies while comparing the simulated results with the measured results of the fabricated antenna. The shift in the resonant frequencies is maybe due to the abnormalities in the antenna fabrication and irregularities in soldering the SMA connector with the antenna. The first band of measured frequencies is in the range of 2.75 GHz to 3.17 GHz which satisfies the WiMAX wireless standard and maritime radio navigation wireless applications. The first resonant frequency band has a bandwidth of 400 MHz. The second set of measured frequencies ranges from 5.79 GHz to 6.28 GHz which encapsulates the ISM wireless standard as well as the dedicated short-range communication (DSRC) used in vehicle-to-vehicle communication. The second resonant frequency set has a bandwidth of 490 MHz. The third range of measured frequencies is from 6.81 GHz to 7.23 GHz which shall be used in the Sub-7 GHz wireless communication frequency range used in fifth-generation (5G) communication. The third resonant frequency range has a bandwidth of 420 MHz. The simulated

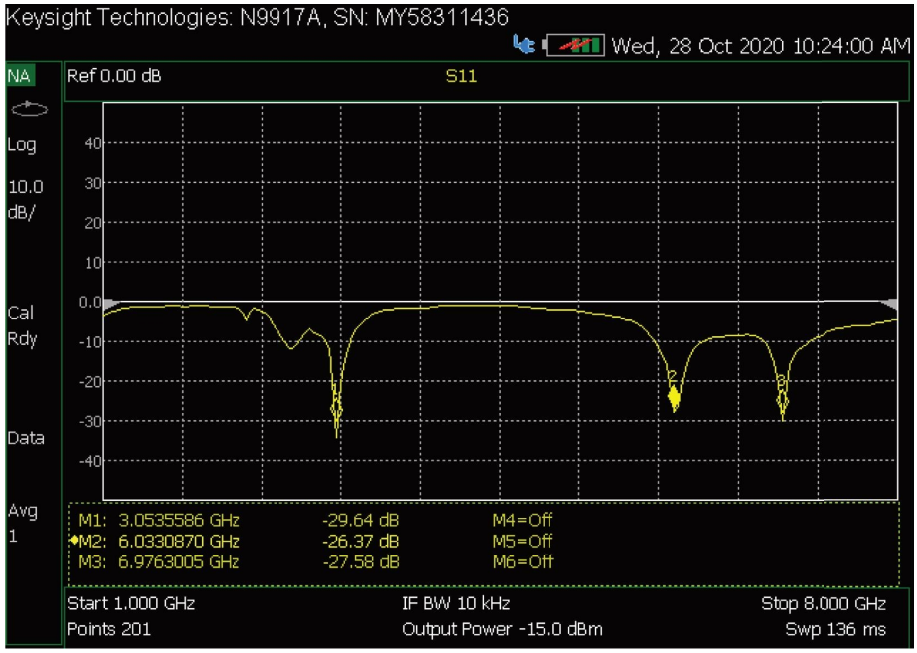

Figure 14: Measured return loss plot of the fabricated antenna structure.

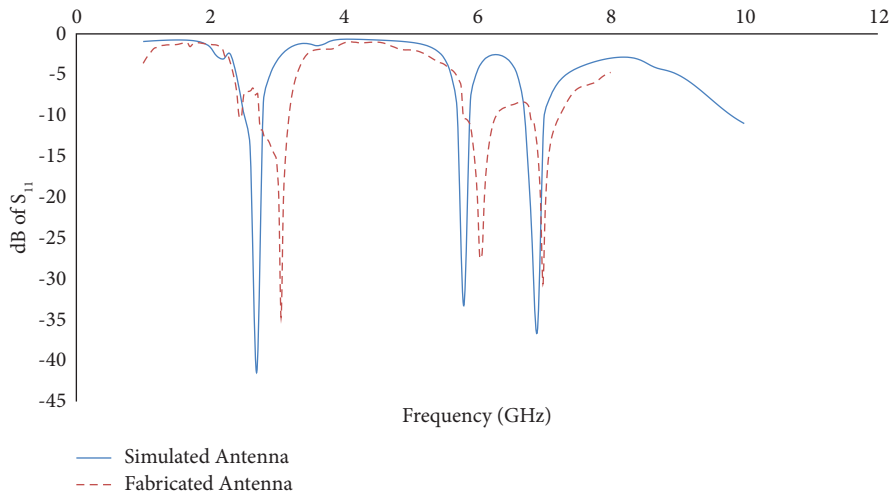

Figure 15: Comparison of return loss values of the simulated and fabricated antenna.

and measured gain values of the proposed antenna structure are shown in Figure 16. The measured gain values are 2.79 dBi at 3 GHz frequency, 2.51 dBi at the frequency of 6 GHz, and 2.64 dBi at 7 GHz frequency. Table 4 provides a comparison of the proposed work with the existing works available in the literature. Hence, the designed antenna is validated for the WiMAX, ISM, and Sub-7 GHz wireless applications.

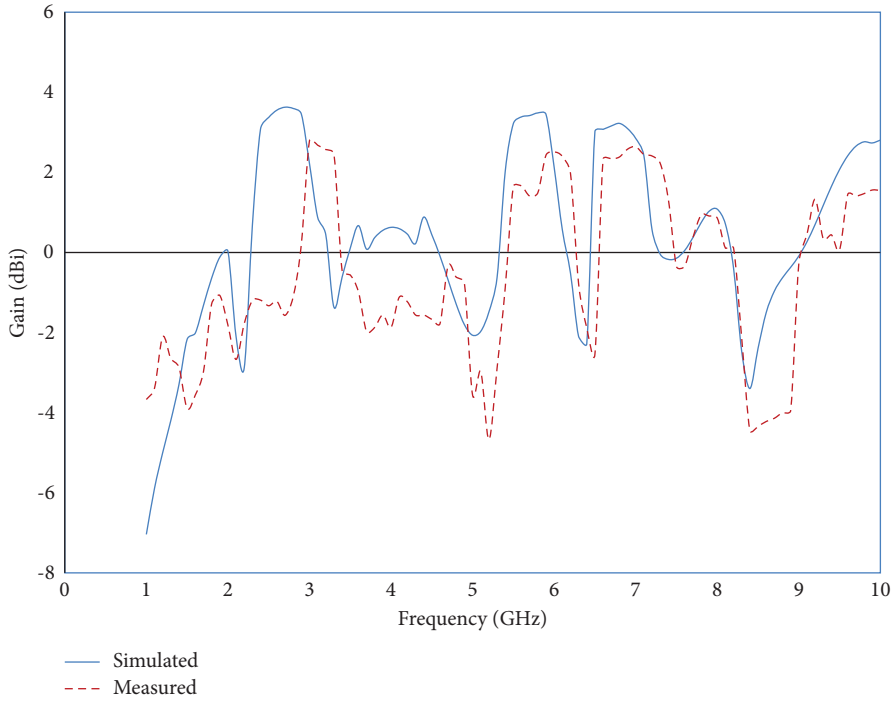

Figure 16: Gain of the simulated and fabricated antenna.

Table 4: Performance comparison of the proposed antenna with the existing work.

Ref	Technique used	Size (mm^3)	Material and permittivity	Gain (dBi)	Bandwidth (MHz)	Number of frequency band	Resonant frequencies (GHz)	Return loss (dB)
[5]	Defected ground plane	$83 \times 56 \times 1.56$	FR4, 4	3.88, 3.87 & 3.83	380, 190 & 300	3	2.47, 3.55 & 5.55	20.8, 14.9 & 17.3
[11]	SRR–CSRR–SIW rectangular resonator antenna based on a composite right/left-handed transmission line	$24.5 \times 30 \times 0.508$	Rogers RT/Duroid 5880, 2.2	5.33 & 5.25	30 & 80	2	5.26 & 9.11	16 & 19
[12]	Defective ground structure	$34 \times 30 \times 1.6$	FR4, 4	2.017, 2.994 & −3.362	190, 120 & 90	3	2.40, 3.50 & 5.80	15.4, 12.8 & 15.2
[18]	Composite right/Left handed transmission line based antenna	$34.1 \times 9.9 \times 1.6$	FR4, 4	1.51 & 1.94	200 & 610	2	2.72 & 5.51	25, 33
[20]	7 element antenna structure	$32 \times 32 \times 0.79$	Rogers RT 5880, 2.2	3.90	1400	1	3.592	46.78
[21]	Sigma shaped patch and slotted ground plane	$29 \times 29 \times 1.6$	FR4, 4	4.76	190	1	5.8	21
Proposed	Defective microstrip structure, defective ground structure	$35 \times 35 \times 1.6$	FR4, 4	2.79, 2.51 & 2.64	400, 490 & 420	3	3, 6 & 7	29.64, 26.37 & 27.58

5. Conclusion

A low-profile triband microstrip patch antenna for WiMAX, ISM, and Sub-7 GHz wireless applications is designed and tested. This paper presents a triple band antenna owing to the multiple resonators employed at the patch of the antenna. Triband characteristics are introduced in the antenna without increasing the size of the antenna. The ground plane is modified to improve the triband radiation characteristics. The modified SRR structure is introduced in the top portion of the patch, and the modified CSRR structure is followed in the ground plane for miniaturization. The measured peak gain observed from the radiation characteristics of the proposed antenna structure is 2.79 dBi. Antenna radiation efficiency at 3 GHz is 88.12%, 6 GHz is 80.19%, and 7 GHz is 82.23%. The compact size and the triband characteristics of the antenna make it suitable for the handheld wireless communication devices.

Data Availability

The data used to support the findings of this study are included within the article.

Conflicts of Interest

The authors declare that they have no conflicts of interest.

References

[1] P. K. Malik and S. Padmanaban, *Microstrip Antenna Design for Wireless Applications*, CRC Press, Boca Raton, FL, USA, 2021.

[2] A. K. Al-azzawi and K. Alaa, "New design approach of a '2.4 Ghz' slotted rectangular patch antenna with a wideband harmonic suppression," *Arabian Journal for Science and Engineering*, vol. 46, no. 10, pp. 9771–9781, 2021.

[3] T. Krishnan, S. Sankar, and V. Ravi, "A dual-band circular patch antenna using hexagon-shaped slots," *International Journal of Communication Systems*, vol. 35, 9 pages, 2022.

[4] P. Dawar, N. S. Raghava, and A. De, "UWB metamaterial-loaded antenna for C-band applications," *International Journal of Antennas and Propagation*, vol. 2019, Article ID 6087039, 13 pages, 2019.

[5] A. Pandya, T. K. Upadhyaya, and K. Pandya, "Tri-band defected ground plane based planar monopole antenna for wi-fi/WIMAX/WLAN applications," *Progress in Electromagnetics Research C*, vol. 108, pp. 127–136, 2021.

[6] A. Jafargholi, A. Jafargholi, and B. Ghalamkari, "Dual-band slim microstrip patch antennas," *IEEE Transactions on Antennas and Propagation*, vol. 66, 6825 pages, 2018.

[7] M. M. Rahman, M. S. Islam, H. Y. Wong, T. Alam, M. T. Islam, and M. T. Islam, "Performance analysis of a defected ground-structured antenna loaded with stub-slot for 5G communication," *Sensors*, vol. 19, p. 2634, 2020.

[8] V. Sharma, N. Lakwar, N. Kumar, and T. Garg, "Multiband low-cost fractal antenna based on parasitic split ring resonators," *IET Microwaves, Antennas & Propagation*, vol. 12, pp. 913–919, 2018.

[9] Z. Xu, Q. Zhang, and L. Guo, "A compact 5G decoupling MIMO antenna based on split-ring resonators," *International Journal of Antennas and Propagation*, vol. 2019, Article ID 3782528, 10 pages, 2019.

[10] C. Feng, Y. Kang, L. Dong, and L. Wang, "High-gain sir dual-band antenna based on CSRR-enhanced SIW for 2.4/5.2/5.8 Ghz wlan," *International Journal of Antennas and Propagation*, vol. 2020, pp. 1–10, 2020.

[11] L. He, S. Yi, and H. Yang, "High-efficiency compact SRR–CSRR–SIW antenna based on CRLH-TL," *Journal of Electromagnetic Waves and Applications*, vol. 36, no. 1, pp. 69–82, 2022.

[12] A. Ibrahim, N. Arina Fazil, and R. Dewan, "Triple-band antenna with defected ground structure (DGS) for WLAN/WiMAX applications," *Journal of Physics: Conference Series*, vol. 1432, Article ID 012071, 2020.

[13] W. Wang, Y. Wang, S. Lou, S. Zhang, and Y. Zhou, "Effect of ground plane deformation on electrical performance of air microstrip antennas," *International Journal of Antennas and Propagation*, vol. 2020, pp. 1–12, 2020.

[14] A. Joe D, T. Krishnan, and T. Krishnan, "A modified sierpinski carpet antenna structure for multiband wireless applications," *The Scientific Temper*, vol. 14, pp. 398–404, 2023.

[15] J. Kukreja, D. K. Choudhary, and R. K. Chaudhary, "A short-ended compact metastructure antenna with interdigital capacitor and U-shaped strip," *Wireless Personal Communications*, vol. 108, no. 4, pp. 2149–2158, 2019.

[16] S. kumar, G. Thangavel, S. A. S. A. I. Ismaili, and B. Subramanian, "MIMO-CSRR Antenna for ISM Band Applications," 2021, https://europepmc.org/article/ppr/ppr337539.

[17] S. Nelaturi and N. V. S. N. Sarma, "CSRR based patch antenna for wi-fi and wimax applications," *Advanced Electromagnetics*, vol. 7, pp. 40–45, 2018.

[18] N. Mishra, A. Chandra, D. Kumar Choudhary, and R. Kumar, "CRLH-TL based dual-band miniaturized antenna for Microwave communication," in *Proceedings of the 2022 IEEE Conference on Interdisciplinary Approaches in Technology and Management for Social Innovation (IATMSI)*, Madhya Pradesh, India, June 2022.

[19] D. K. Choudhary, N. Mishra, P. K. Singh, and A. Sharma, "Miniaturized power divider with triple-band filtering response using coupled line," *IEEE Access*, vol. 11, pp. 27602–27608, 2023.

[20] L. C. Paul, S. S. A. Ankan, T. Rani et al., "A wideband highly efficient omnidirectional compact antenna for WiMAX/lower 5G communications," *International Journal of RF and Microwave Computer-Aided Engineering*, vol. 2023, Article ID 7237444, 10 pages, 2023.

[21] Das, T. Kumar, D. P. Mishra, and S. Kumar Behera, "Slotted microstrip antenna for 5.8 ghz ism band applications," in *Proceedings of the 2019 International Conference On Range Technology (ICORT)*, Balasore, India, February 2019.

[22] M. S. Singh and R. Mishra, "Rectangular monopole patch antenna for c-band and x-band applications," in *Proceedings of the 2018 5th IEEE Uttar Pradesh Section International Conference On Electrical, Electronics And Computer Engineering (UPCON)*, Uttar Pradesh, India, August 2018.

[23] J. Gomez-Ponce, D. Burghal, N. A. Abbasi et al., "Directional delay spread and interference quotient analysis in sub-7ghz wi-fi bands," in *Proceedings of the GLOBECOM 2020-2020 IEEE Global Communications Conference*, pp. 01–06, IEEE, Taipei, Taiwan, December 2020.

[24] E. Jarauta, J. C. Iriarte, F. Falcone, and F. F. Lanas, "Characterization of multilayer coupling based on square complementary split ring resonator for multiport device implementation," *Micromachines*, vol. 14, no. 1, p. 68, 2022.